The numerical-instrumental method development for hard-to-reach industrial facilities and products infrared thermography testing

VIKTOR HLUKHOVSKYI, VALENTYN LYTVYNENKO
E.O.Paton Electric Welding Institute (PWI), 11,
Kazymyr Malevych St., Kyiv, 03150, UKRAINE

Abstract: To increase the efficiency of remote monitoring of the condition of hard-to-reach areas of industrial structures and products, a numerical and instrumental approach to infrared thermography monitoring has been developed. It consists of the complex use of industrial thermal imaging devices and computational methods for analyzing temperature fields in the structures under study. This allows improving the accuracy of determining the geometric features of defects and reducing the complexity of work on technical diagnostics of the condition. The use of the developed approach is demonstrated on typical examples of non-contact monitoring of the technical condition of industrial chimneys.

Keywords: infrared thermography testing, industrial objects and products, thermophysical parameters, defect, numerical-instrumental method, industrial chimneys.

Received: March 29, 2024. Revised: November 24, 2024. Accepted: December 23, 2024. Published: March 5, 2025.

1. Introduction

Among industrial facilities that undergo long operational cycles, a separate group includes hard-to-reach and potentially dangerous ones, which are characterized by operation in extreme thermal and physical conditions. Such facilities are mainly concentrated in the energy, metallurgical, machine-building, chemical and petrochemical industries, as well as in construction and municipal services.

The most common among them are process pipelines and tanks, industrial chimneys and gas ducts, which are an integral part of the technical schemes of industrial enterprises and which, to one degree or another, have a multilayer cylindrical wall shape.

Industrial chimneys are typical structures with a multilayer wall. These are complex and high-cost high-rise structures, the main function of which is to remove flue gases and disperse them in the atmosphere, as the final link in technological processes. The problem of most of them is the exhaustion of the operational resource and requires measures to extend it.

One of the ways to solve this problem is to estimate the residual resource using non-destructive testing and technical diagnostics methods by creating new, improved methods that would allow remote and prompt receipt of information about the reliability characteristics of the above objects.

For the analysis of this class of structures, when detecting anomalies of various types, the infrared thermography method has shown its effectiveness, which allows for remote diagnostics of the condition of objects in hard-to-reach places and reduces production risks for personnel [1, 2]. The essence of the method is that the temperature difference inside the studied structure and outside is different, which causes a certain warming of the outer surface. The actual surface temperature distribution depends on many factors, in particular, on the thermal resistance of the structure, thermal conductivity of materials, and also on the presence of operational defects, i.e. local thinning or cavities in the wall. This can be recorded using non-contact thermography

methods. The simplicity and accessibility of this approach has led to its widespread use for assessing the thermal characteristics of objects, identifying areas of excessive heat loss, air leaks, lack or damage to thermal insulation, sources of moisture, etc. [3, 4]. The non-contact nature of infrared testing allows it to be widely used for analyzing the destruction of metallic materials, as well as for detecting subsurface defects in polymers or composites [5].

The vast majority of works in the direction of passive thermography were related to solving the problem of thermal imaging defectoscopy by developing one-dimensional models of defect-free walls stationary temperature fields or obtaining reference temperature distributions on the surface of laboratory samples [6-7].

But one of the fundamental disadvantages of this method of technical diagnostics is the low accuracy of quantitative assessment of the sizes of detected defects, especially along the thickness of the structure. This means that in the case of detecting certain anomalies, additional measures are required to examine the corresponding structural element for a substantiated expert conclusion on their admissibility, which, to some extent, negates the advantages of infrared testing. Therefore, the development of science-intensive approaches to analyzing the results of measuring temperature fields from the point of view of their quantitative interpretation is relevant. The purpose of this work is to develop a numerical and instrumental method for the thermal condition of large-sized structures and buildings based on the integrated use of thermal imaging devices and computational approaches to the analysis of thermal fields.

2. Materials and Methods

The instrumental part of the proposed technique takes place in the thermographic measurement of natural (passive thermography) or induced (active thermography) temperature fields on surfaces. Areas of surface or subsurface defects are characterized by a local change in temperature. At the same time, the same temperature in the area of the defect and in the defect-free part of the structure depends, first of all, on the residual wall thickness and the type of defect. Such dependencies were obtained on the basis of the numerical calculation of the temperature field, taking into account the geometric and physical features of the structure state. The mathematical models and means of their computer implementation validation was carried out on the basis of relevant laboratory studies of model structural elements.

The most adequate mathematical formulation of a multilayer wall IR thermography problem is the non-stationary three-dimensional equation of thermal conductivity, which describes the heat transfer in the layers of the product [8]:

$$a_j \nabla^2 T_j = \partial T_j / \partial \tau,\ j = 1,...,n \qquad (1)$$

where T_j is the absolute temperature of the j-th layer.

The conditions of heat exchange on the external surfaces of the product when heated by an external heat source and cooled by convection and radiation can be represented as follows:

$$T_j(\tau = 0) = T_0 \qquad (2)$$

where T_0 is the initial control temperature; qi – generalized coordinate; Q – heat flow density; ε_j is the effective radiation coefficient of the outer surface of the j-th layer; σ is the Stefan-Boltzmann constant.

The condition of continuity of temperature and heat flows at the internal boundaries of solid layers will have the form:

$$T_j = T_k, \lambda_i(\partial T_j / \partial q_i) = \lambda_k(\partial T_k / \partial q_i) \qquad (3)$$

at the boundaries of the solid layer - a gaseous defect, taking into account the radiation of the defect walls, takes the form:

$$T_j = T_k, \lambda_i(\partial T_j / \partial q_i) = \lambda_k(\partial T_k / \partial q_i) - \varepsilon_{ik}\sigma(T_j^4 - T_k^4) \qquad (4)$$

where ε_{jk} is the coefficient of mutual irradiation of the layers.

The calculation of the non-uniform temperature field (1) was based on the finite-difference solution of the non-stationary heat conduction equation [9,10,11]:in the Cartesian coordinate system (x, y, z) – to describe heat transfer processes in plates:

$$C\rho(x,y,z,T)\cdot\frac{\partial T(x,y,z,t)}{\partial t}=\frac{\partial}{\partial x}\left[\lambda(x,y,z)\cdot\frac{\partial T(x,y,z,t)}{\partial x}\right]+ \\ +\frac{\partial}{\partial y}\left[\lambda(x,y,z)\cdot\frac{\partial T(x,y,z,t)}{\partial y}\right]+\frac{\partial}{\partial z}\left[\lambda(x,y,z)\cdot\frac{\partial T(x,y,z,t)}{\partial z}\right]. \quad (5)$$

cylindrical coordinate system (r, β, z) – for cylindrical structures:

$$C\rho(r,\beta,z,T)\cdot\frac{\partial T(r,\beta,z,t)}{\partial t}=\frac{1}{r}\cdot\frac{\partial}{\partial r}\left[r\cdot\lambda(r,\beta,z)\cdot\frac{\partial T(r,\beta,z,t)}{\partial r}\right]+ \\ +\frac{1}{r^2}\cdot\frac{\partial}{\partial\beta}\left[\lambda(r,\beta,z)\cdot\frac{\partial T(r,\beta,z,t)}{\partial\beta}\right]+\frac{\partial}{\partial z}\left[\lambda(r,\beta,z)\cdot\frac{\partial T(r,\beta,z,t)}{\partial z}\right]. \quad (6)$$

where T is temperature, °C; λ – thermal conductivity, J/(m·s·°C); $C\rho$ – volumetric heat capacity, J/(m^3·°C).

When setting the problem (5) or (6), boundary conditions of the second kind were used in accordance with the combined effect of characteristic heat sources and drains.

The numerical solution of the heat conduction equation made it possible to determine both the stationary temperature distribution and the kinetics of the development of the temperature field, which was important in the laboratory verification of the reliability of the numerical approach.

3. Results

The developed approach was verified by comparing the temperature fields measured using a thermal imager, with the matrix resolution of 320×240 pixels, on test samples with model defects, with the results of numerical calculations. Metal plates with dimensions of 300×200×10 mm and 260×125×10 mm made of St3 kp steel were used as test samples (fig. 1).

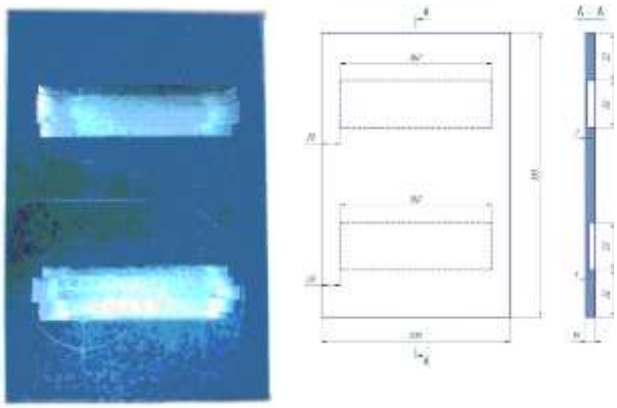

a

Fig. 1. Appearance and schemes of plates with model defects used for laboratory research: a – plate with thinning; c – plate with delamination

The thermophysical properties of the material depending on the temperature are shown in Table 1.

TABLE 1
St3 kp steel thermophysical properties on temperature Dependence [12]

T, °C	Thermal conductivity, W/(m °C)	Heat capacity, J/(kg °C)
100	55	482
200	54	498
300	50	514
400	45	533
500	39	555
600	34	584
700	30	626

Samples were heated at different time intervals. Thus, the sample was heated with dilutions for 905 seconds in order to achieve a transition from a non-stationary temperature regime to a stationary one (Fig. 2).

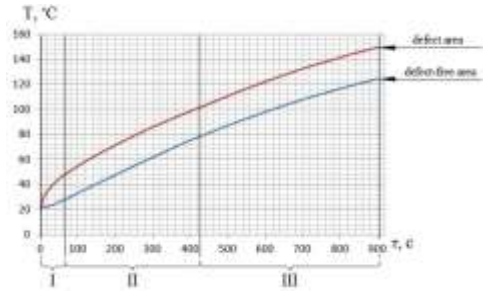

Fig. 2. The nature of the experimental temperature changes over the defective and non-defective areas depending on time

Shown in fig. 2 temperature distribution for a plate with thinning, divided into three sectors: sector I corresponds to the time interval from 0 to 65 with heating, in which both embedded defects appear as separate temperature maxima; Sector II corresponds to the time interval of heating from 65 to 425 s, when one temperature maximum appears, the corresponding defect with the greatest depth of occurrence; The III sector corresponds to the time interval of heating from 425 s to 905 s and even more, the amount of the temperature maximum shifts in the zone between the defects and corresponds to the overheated defect-free area.

The surface thermograms of the laboratory sample with wall thinning are shown in fig. 3.

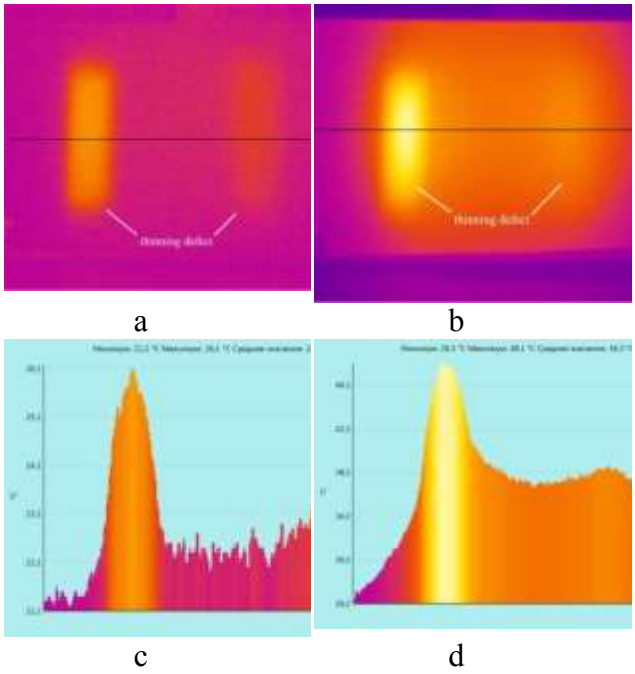

Fig. 3. Temperature fields thermograms of on the of a flat laboratory sample surface model thinning defects (a, c) and temperature distributions along the P1 line (b, d) at different time intervals after the start of heating: a, b – 5 s; c, d - 65 p

The one-dimensional calculated temperature distributions with the corresponding values of the experimentally obtained temperature maxima above the wall thickenings shows in Fig. 4.

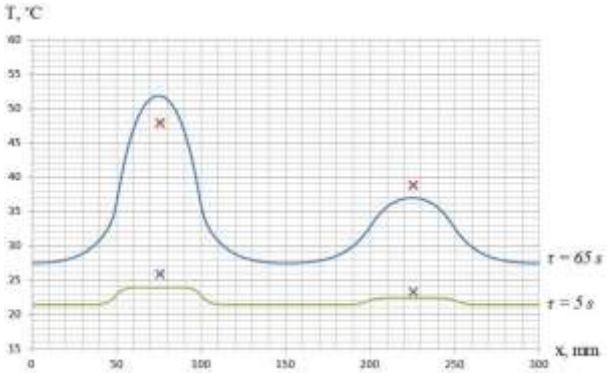

Fig. 4. Calculated one-dimensional temperature distributions with the corresponding values of the experimentally obtained temperature maxima over the thinning of the wall for different periods of heating time

The sample with internal heterogeneity of the delamination type was heated for 47 seconds with fixation of its surface temperatures, the infrared images of which are shown in Fig. 5.

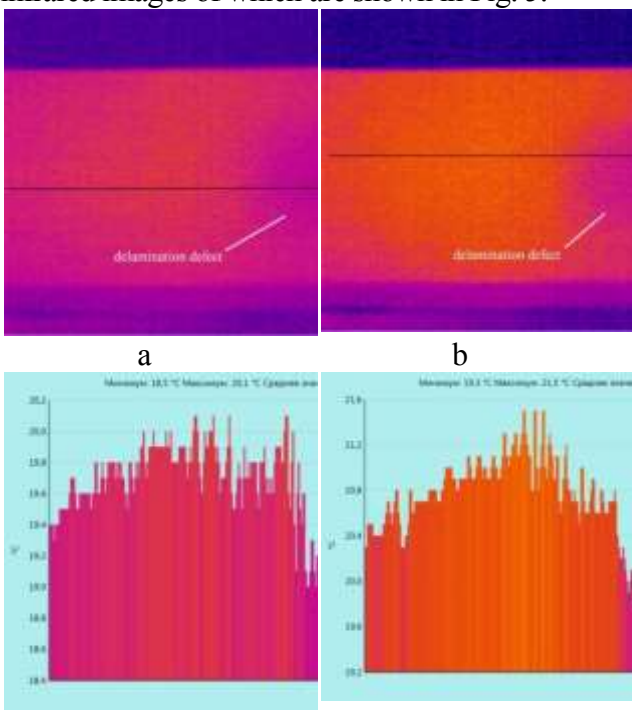

Fig. 5. Thermograms of temperature fields on the surface of a flat laboratory sample with a model delamination defect (a, c) and temperature distributions along the P1 line (b, d) at different time intervals after the start of heating: a, b – 18 s; c, d - 47 p

For those shown in fig. 5 temperature distributions, corresponding mathematical models were created, the calculated one-dimensional temperature distributions of which, with the corresponding values of the experimentally obtained temperature minima above the delamination of the plate are shown in fig. 6.

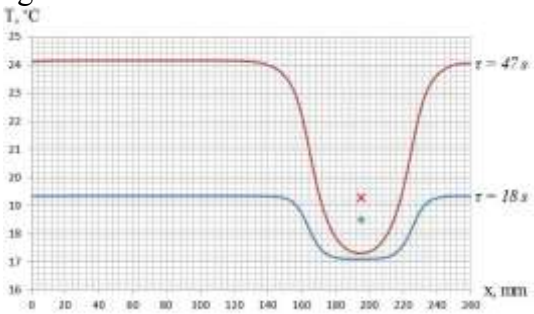

Fig. 6. Calculated one-dimensional temperature distributions with the corresponding values of the experimentally obtained temperature maxima above the delamination for different periods of heating time

As can be seen from the measurement results, the areas of thinning are characterized by a local increase in temperature compared to the periphery from 3 to 22 °C, depending on the depth of the defect and the heating time. In contrast to the thinning of the plate, in the case of delamination, a local decrease in temperature is observed on the surface of the laboratory sample as a result of an increase in the thermal resistance of the defect. For the case considered as part of laboratory studies of a plate with delamination and heating for 47 s, the value of the local decrease in surface temperature was about 2 °C.

Comparisons of experimentally measured temperature distributions with the results of calculations show an error of no more than 15% both during the heating stage and in the stationary mode. This level of accuracy is sufficient for solving engineering problems of technical diagnostics and for increasing the accuracy of quantitative analysis of the corresponding IR images.

4. Discussion

The developed approach was used to increase the efficiency of diagnosing the technical condition of typical industrial chimneys using the example of a reinforced concrete four-layer industrial chimney design for PTVM-100 boiler units (peak heating hot water gas-oil boiler) (Fig. 8). The height of the pipe is 120 m, the inner diameter of the mouth is 5900 mm.

Fig. 8. General view of the industrial chimney 120 for PTVM-100 boiler units

Let the chimney control area with an outer diameter of 7444 mm be located at a height of 60 to 65 meters. The thermophysical characteristics of the chimney layers materials are given in Table 2.

TABLE 2
Thermophysical properties of materials of different layers of an industrial chimney for PTVM-100 boiler units in a dry state at atmospheric pressure and a temperature of 20...110 °C [13]

Layer name	Material	Average thickness, mm	Thermal conductivity, W/(m °C)	Heat capacity, J/(kg °C)
Lining	Brick red solid	120	0,74	860
Thermal insulation	Mineral wool	50	0,041	920
Pressure brick	Brick red solid	120	0,74	860
Reinforced concrete trunk	Reinforced concrete	220	1,70	840

Let's determine the temperature for a defect-free chimney for operating conditions when the temperature of the gases in the middle of the barrel is 106 °C, and the temperature of the outside air is 8 °C, using the classic one-dimensional model of the stationary temperature field and the numerical-instrumental method (Fig. 9) [14].

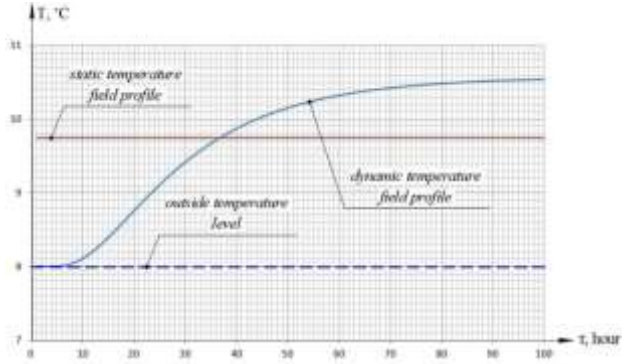

Fig. 9. Defect-free chimney surface temperature

Figure 9 shows that the dynamic temperature profile turns into a static one within 90 hours and reaches a value of 10.54 °C. At the same time, the value of the static temperature field is 9.75 °C. Thus, the difference between the temperatures of the static and dynamic temperature fields differs by 11.3% , which is quite acceptable for the use of the numerical-instrumental method in further calculations.

Let's consider the most typical case, when the humidity of the inner chimney's layers is increased (Tab. 3). Let's determine the temperature distributions for cases when the linear dimensions of the defect vary from 4 to 1 meter. (Fig. 10)

TABLE 3
Thermophysical properties of materials of different layers of an industrial chimney for PTVM-100 boiler units in a humidity state at atmospheric pressure and a temperature of 20... 110 °C [15, 16]

Layer name	Material	Average thickness,	Thermal conductivity, W/(m	Humidity, %

		mm	°C)	
Lining	Brick red solid	120	1,910	22
Thermal insulation	Mineral wool	50	0,398	75
Pressure brick	Brick red solid	120	1,910	22
Reinforced concrete trunk	Reinforced concrete	220	2,464	4

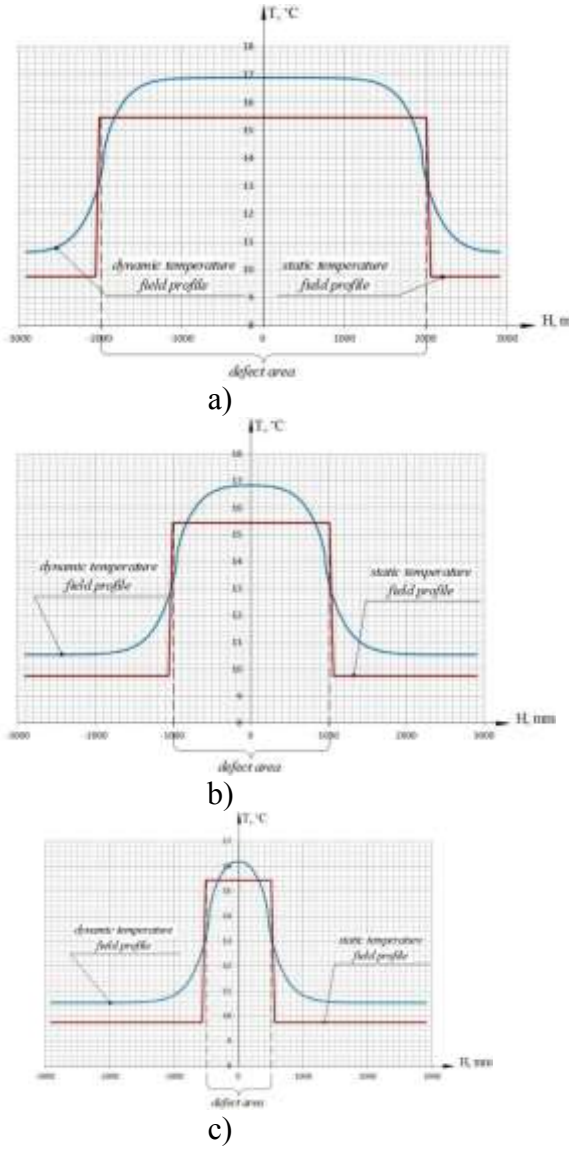

Fig. 10. Temperatures above defects in the body of the chimney trunk with linear dimensions: a) 4000 mm; b) 2000 mm; c) 1000 mm

Fig. 10 shows that the temperature above the defect, obtained by the numerical-instrumental method, also differs from the temperature of the classical one-dimensional model of the stationary temperature field.

The proposed calculation dependencies allow for a more accurate analysis of the corresponding thermograms, an estimation of the temperature inside the pipe at a certain height (the corresponding dependencies converge to specific surface temperatures of a defect-free area with a defect size equal to zero), and a determination of the type and size of defects in the infrared testing process.

5. Conclusion

- A numerical-instrumental method of thermographic analysis of the technical condition of large-sized structures and structures was developed, with the indication of increasing the accuracy of determining the size of operational defects. For this, the methods of numerical modeling of the non-uniform temperature field on the surface of flat or cylindrical control objects are combined with instrumental approaches of thermographic analysis of infrared radiation.
- To verify the reliability of the developed method, laboratory studies were conducted on steel plates with model defects - local thinning and internal delamination. According to the results of calculations and thermographic measurement of the surface temperature of the defective sample, the error of the developed approach is shown to be no higher than 15%.
- On the example of a reinforced concrete four-layer industrial cnimney for PTVM-100 boiler

units with a height of 120 meters and an inner diameter of the mouth of 5900 mm, was performed a comparative analysis of the numerical-instrumental method and the classical one-dimensional model of the stationary temperature field for a defect-free chimney trunk and for a trunk with the same type of defects of different lengths.

- It was established that in the case of a defect-free chimney's trunk, the numerical-instrumental method in comparison with the classical one-dimensional model of stationary temperature fields gives overestimated temperature values within 11.3%, and for a defect-free wall, these values do not exceed 10.94% and decrease as the linear size of the defect decreases.
- The obtained deviation indicators are acceptable for the application of the numerical-instrumental method for calculating reference temperatures of both defect-free and defective walls of industrial facilities, especially when there is a change in external temperatures during the day.

References

[1]. Glukhovskiy V.Yu., Bondarenko O.G. Features of diagnostics of technical condition of industrial flue pipes by passive thermal imaging method. Technical Diagnostics and Non-Destructive Testing, 2019, №03. P. 36-45.

[2]. Glukhovskiy V.Yu. The IR thermography application for the technical condition industrial smoke pipes monitoring. Technical Diagnostics and Non-Destructive Testing, 2015, №01. P. 55-59.

[3]. Vavilov V.P., Shiryaev V.V., Nesteruk D.A. Application of Fourier analysis and the method of component analysis for processing dynamic thermal control data // Izvestia TPU. 2008. No. 2. P. 279-285. [in Russian].

[4]. Vavilov V.P., Nesteruk D.A. Active thermal inspection of composite materials with the use of neural networks //Russion Jornal of Nondestructive Testing. 2011. Vol. 2011. P. 655-662.

[5]. Momot A.S., Galagan R.M., Glukhovskii V.Yu. Deep Learning Automated System of Thermal Defectometry of Multilayer Materials: / // Devices and Methods of Measurements – 2021, vol. 12, no 2, P. 98-107.

[6]. Sendkowski J., Tkaczyk A., Tkaczyk L. Termowizja i termografia w diagnostyce kominów przemysłowych. Przykłady, możliwości. PRZEGLĄD BUDOWLANY 2/2013. – P. 21-25.

[7]. Maj M., Ubysz A., Hammadeh H., Askifi F., Non-Destructive Testing of Technical Conditions of RC Industrial Tall Chimneys Subjected to High Temperature. *Materials* 2019, *12*(12), 2027. P. 1-15.

[8]. Maslova V.A., Storozhenko V.A. Thermography in diagnostics and non-destructive testing. Kharkov: “SMIT Company”, 2004. – 160 p. [in Russian].

[9]. Akhonin S.V., Milenin A.S. and Pikulin A.N. Modeling of processes of evaporation of alloying elements in EBSM of cylindrical ingots produced from Ti-base alloys. *Problemy Spetsial'noj Electrometallurgii*. 1. 2005. P. 21-25.

[10]. Milenin O.S., Glukhovskyi V.Yu., Velykoivanenko O.A., Lytvynenko V.A. Numerical-instrumental method of thermographic control of the state of large-sized structures and constructions.Technical Diagnostics and Non-Destructive Testing #3, 2023, pp. 10-15

[11]. Karkhin, V.A. Thermal Processes in Welding. Singapore: Springer Singapore. 2019. 491 p.
[12]. (1991) Physical quantities. Handbook. Eds by I.S. Grigoriev, E.Z. Mejlikhov. Moscow, Energoatomizdat [in Russian].
[13]. DBN B.2.6-31:2006.Thermal insulation of buildings. Minestru of bilding of Ukraine. Kyiv 2006, 15 p. [in Ukrainian].
[14]. Troitskiy V. Hlukhovskyi V.Thermographic assessment of defects in industrial facilities and products. Materials Evaluation 82 (12): p. 42–50.
[15]. Malarenko V.A., Gerasimova O.M., Maleev O.I. Building thermal physics. A course of lectures for students of all forms of education in construction specialties. – Kharkiv: NUUEKh, 2007. – 100 p.
[16]. Antepara I., Fiala L., Pvlik Z., Cerny R. Moisture Dependent Thermal Properties of Hydrophilic Mineral Wool: Application of the Effective Media Theory. ISSN 1392–1320 MATERIALS SCIENCE (MEDŽIAGOTYRA). Vol.21, No. 3. 2015, 449-454 p..